



Newly Discovered Antimicrobial Peptide Scyampcin_{44–63} from *Scylla paramamosain* Exhibits a Multitargeted Candidacidal Mechanism *In Vitro* and Is Effective in a Murine Model of Vaginal Candidiasis

Ying Zhou,^a Xiangyu Meng,^a Fangyi Chen,^{a,b} Ming Xiong,^{a,b} Weibin Zhang,^a Ke-Jian Wang^{a,b}

^aState Key Laboratory of Marine Environmental Science, College of Ocean and Earth Sciences, Xiamen University, Xiamen, China

^bState-Province Joint Engineering Laboratory of Marine Bioproducts and Technology, College of Ocean and Earth Sciences, Xiamen University, Xiamen, China

ABSTRACT The emergence of azole-resistant and biofilm-forming *Candida* spp. contributes to the constantly increasing incidence of vulvovaginal candidiasis. It is imperative to explore new antifungal drugs or potential substituents, such as antimicrobial peptides, to alleviate the serious crisis caused by resistant fungi. In this study, a novel antimicrobial peptide named Scyampcin_{44–63} was identified in the mud crab *Scylla paramamosain*. Scyampcin_{44–63} exhibited broad-spectrum antimicrobial activity against bacteria and fungi, was particularly effective against planktonic and biofilm cells of *Candida albicans*, and exhibited no cytotoxicity to mammalian cells (HaCaT and RAW264.7) or mouse erythrocytes. Transcriptomic analysis revealed four potential candidacidal modes of Scyampcin_{44–63}, including promotion of apoptosis and autophagy and inhibition of ergosterol biosynthesis and the cell cycle. Further study showed that Scyampcin_{44–63} caused damage to the plasma membrane and induced apoptosis and cell cycle arrest at G₂/M in *C. albicans*. Scanning and transmission electron microscopy demonstrated that Scyampcin_{44–63}-treated *C. albicans* cells were deformed with vacuolar expansion and destruction of organelles. In addition, *C. albicans* cells pretreated with the autophagy inhibitor 3-methyladenine significantly delayed the candidacidal effect of Scyampcin_{44–63}, suggesting that Scyampcin_{44–63} might contribute to autophagic cell death. In a murine model of vulvovaginal candidiasis, the fungal burden of vaginal lavage was significantly decreased after treatment with Scyampcin_{44–63}.

KEYWORDS antimicrobial peptides, Scyampcin_{44–63}, candidacidal mechanism, therapeutic effect, vulvovaginal candidiasis

Vulvovaginal candidiasis (VVC) is the most prevalent candidal infection, mostly occurring in women of childbearing age, and afflicts almost 75% of women at least once in their lifetime, among whom nearly half will experience a recurrence (1, 2). Furthermore, 5% to 8% of adult women suffer recurrent vulvovaginal candidiasis (RVVC), defined as four or more episodes annually. Although VVC is nonlethal, VVC causes discomfort, pain, and social embarrassment along with considerable economic loss, producing approximately \$1.8 billion in medical costs and \$1 billion in additional annual payments in the United States alone (1, 3). Nystatin- or azole-based topical agents are intravaginally applied to treat ordinary *C. albicans* VVC in the United States (3). Fluconazole has become the primary choice for treating VVC because of its high oral bioavailability, convenient drug delivery, and favorable safety properties. However, continuous use or inappropriate usage exacerbates the emergence of fluconazole-resistant *C. albicans* and has greatly hindered clinical therapy (4).

Antimicrobial peptides (AMPs) are considered promising alternatives to antibiotics, as AMPs have multiple modes of action, broad-spectrum activity against pathogens, and a low propensity to produce resistance (5, 6). Most antifungal peptides interact with fungal

Copyright © 2023 Zhou et al. This is an open-access article distributed under the terms of the [Creative Commons Attribution 4.0 International license](https://creativecommons.org/licenses/by/4.0/).

Address correspondence to Ke-Jian Wang, wkjian@xmu.edu.cn.

The authors declare no conflict of interest.

Received 6 January 2023

Returned for modification 31 January 2023

Accepted 18 April 2023

Published 10 May 2023

cell membranes, causing membrane disruption. Some antifungal peptides interfere with cell wall synthesis, while others exert different fungicidal mechanisms, e.g., stimulating reactive oxygen species (ROS) production, dissipating mitochondrial membrane potential, triggering apoptosis, disrupting cation homeostasis, inducing ATP efflux, interfering with the cell cycle, and disrupting autophagy and vacuolar function (5). According to the clinical data shown in the Data Repository of Antimicrobial Peptides (<http://dramp.cpu-bioinform.org/>, accessed on 21 November 2022), 77 AMPs are under clinical trials. However, most of these AMPs have been shown to target against bacterial infections, while only a few are applied for treating candidiasis, including PAC-113 and CZEN-002. Therefore, there is an urgent need to explore new antifungal compounds.

The mud crab *Scylla paramamosain* is a kind of marine crustacean that relies only on the effectors of innate immunity, such as AMPs, against invading pathogens. Frequent exposure to a complex and changing microbial environment makes *S. paramamosain* an arsenal of AMPs. Since 2006, our group has identified various novel AMPs in *S. paramamosain*, such as Scygonadin (7), Scyeprocin (8), Sparamosin₂₆₋₅₄ (9), Sparanegtin (10), and Spampcin₅₆₋₈₆ (11). In the present study, we identified a novel AMP named Scyampcin₄₄₋₆₃ from the mud crab *S. paramamosain*. Considering that *C. albicans* is the most prevalent human fungal pathogen and that Scyampcin₄₄₋₆₃ has potent anti-candidal activity, we performed RNA sequencing (RNA-seq) to reveal the potential candidacidal mechanism of Scyampcin₄₄₋₆₃ and verified it in experiments. We further evaluated the possibility of clinical application by exploring the efficacy of Scyampcin₄₄₋₆₃ *in vivo*.

RESULTS

Cloning and bioinformatics analysis. Based on the transcriptional database of *S. paramamosain* established by our research group, we screened and cloned a new functional gene that had no similarity in nucleotide or amino acid sequence with the existing online database, and named it Scyampcin (GenBank accession number [MW388710](#)). The full-length cDNA of Scyampcin consists of a 5'-untranslated region (UTR) of 132 bp, an open reading frame (ORF) of 213 bp, and a 3'-UTR of 144 bp (excluding the poly[A] tail) (Fig. S1A). Scyampcin encodes 70 amino acid residues, with a calculated mass of 8.2 kDa and an estimated isoelectric point (pI) of 10.11. The predicted secondary and tertiary structures showed that Scyampcin contained α -helices and β -sheets (Fig. S1B and C). According to the predicted antimicrobial region within peptides in the CAMP_{R3} database, we synthesized the C-terminal amidated truncated peptide Scyampcin₄₄₋₆₃. The physicochemical parameters of Scyampcin₄₄₋₆₃ are shown in Fig. S1D. Scyampcin₄₄₋₆₃ contains 20 amino acids and is rich in lysine (Lys, 30%) and phenylalanine (Phe, 15%), with a hydrophobic ratio of 21.1% and a net charge of +6.

Scyampcin₄₄₋₆₃ exhibits potent antimicrobial activity. The antimicrobial activities of Scyampcin₄₄₋₆₃ were determined as shown in Table 1. Scyampcin₄₄₋₆₃ showed broad-spectrum antimicrobial activity against Gram-positive bacteria (*Staphylococcus aureus*, *Bacillus subtilis*, *Bacillus cereus*, *Staphylococcus epidermidis*, *Listeria monocytogenes*, *Enterococcus faecium*, and *Enterococcus faecalis*), Gram-negative bacteria (*Shigella flexneri*, *Acinetobacter baumannii*, *Escherichia coli*, and *Pseudomonas aeruginosa*), and fungi (*Cryptococcus neoformans*, *Candida albicans*, *Candida tropicalis*, *Candida parapsilosis*, *Candida krusei*, *Fusarium graminearum*, and *Fusarium solani*). The minimum bactericidal concentration (MBC) or minimum fungicidal concentration (MFC) values of Scyampcin₄₄₋₆₃ for all of the tested microorganisms were below 6 μ M, except for the MBC of 12 to 24 μ M for *P. aeruginosa*. Even when the concentrations of Scyampcin₄₄₋₆₃ reached 96 μ M, Scyampcin₄₄₋₆₃ was safe for mammalian HaCaT or RAW264.7 cells and was without hemolytic activity toward mouse erythrocytes (Fig. S2).

Transcriptomic analysis of *C. albicans*. (i) Analysis and verification of differentially expressed genes (DEGs). We performed a transcriptomic analysis of untreated and Scyampcin₄₄₋₆₃-treated *C. albicans* to gain further insight into the candidacidal mechanism of Scyampcin₄₄₋₆₃. After Scyampcin₄₄₋₆₃ treatment, a total of 1,907 DEGs were obtained in *C. albicans*, including 849 upregulated genes and 1,058 downregulated genes (Fig. 1A). The upregulated genes were involved in different biological processes, such as cell wall synthesis, the cell wall integrity (CWI) pathway, antioxidative stress,

TABLE 1 Antimicrobial activities of Scyampcin₄₄₋₆₃^a

Microorganisms	CGMCC no.	MBC or MFC (μM)
Gram-positive bacteria		
<i>Staphylococcus aureus</i>	1.2465	3 to 6
<i>Bacillus subtilis</i>	1.3358	0 to 3
<i>Bacillus cereus</i>	1.3760	3 to 6
<i>Staphylococcus epidermidis</i>	1.4260	0 to 3
<i>Listeria monocytogenes</i>	1.10753	3 to 6
<i>Enterococcus faecium</i>	1.131	0 to 3
<i>Enterococcus faecalis</i>	1.2135	3 to 6
Gram-negative bacteria		
<i>Shigella flexneri</i>	1.1868	0 to 3
<i>Acinetobacter baumannii</i>	1.6769	0 to 3
<i>Escherichia coli</i>	1.2389	0 to 3
<i>Pseudomonas aeruginosa</i>	1.1785	12 to 24
Fungi		
<i>Cryptococcus neoformans</i>	2.1563	0 to 3
<i>Candida albicans</i>	2.2411	3 to 6
<i>Candida tropicalis</i>	2.1975	0 to 3
<i>Candida parapsilosis</i>	2.1846	0 to 3
<i>Candida krusei</i>	2.1875	3 to 6
<i>Fusarium graminearum</i>	3.4521	3 to 6
<i>Fusarium solani</i>	3.584	3 to 6

^aCGMCC, China General Microbiological Culture Collection Center; MBC, minimum bactericidal concentration; MFC, minimum fungicidal concentration.

endoplasmic reticulum (ER) stress, and apoptosis (Fig. 1A; Table S4). The downregulated genes mainly related to ergosterol biosynthesis (Fig. 1A; Table S5). To validate the RNA-seq results, we randomly selected 12 genes, including five upregulated and seven downregulated genes, from the DEG libraries for quantitative reverse-transcription PCR (qRT-PCR) (primers for qRT-PCR are listed in Table S3). The trends of gene expression levels were consistent between qRT-PCR and RNA-seq. Hence, the qRT-PCR results validated the reliability of the RNA-seq data (Fig. 1B).

(ii) KEGG enrichment analysis of DEGs. In response to Scyampcin₄₄₋₆₃ treatment, the KEGG enrichment analysis showed that pathways associated with amino acid metabolism and biosynthesis, biosynthesis of secondary metabolites, 2-oxocarboxylic acid metabolism, autophagy, glycerolipid metabolism, and inositol phosphate metabolism were upregulated, while pathways related to replication and repair, transcription, translation, cell cycle, meiosis, and steroid biosynthesis were downregulated (Table 2). The DEGs enriched in KEGG pathways (autophagy, cell cycle and steroid biosynthesis, corrected P values < 0.05, and $|\log_2[\text{fold change}]| > 1$) were individually subjected to hierarchical clustering analysis, and a heat map was constructed (Fig. 1C). Among these DEGs, 19 of the 25 genes participating in the autophagy pathway were upregulated, and 35 of the 39 genes related to the cell cycle and 9 of the 11 genes associated with steroid biosynthesis were downregulated.

Candidacidal and anti-biofilm activity of Scyampcin₄₄₋₆₃. As Scyampcin₄₄₋₆₃ had potent candidacidal activity, we examined the time-killing curve and the anti-biofilm activity. The candidacidal activity of Scyampcin₄₄₋₆₃ was determined by colony count assays (Fig. 2A). After exposure to 6 μM and 12 μM Scyampcin₄₄₋₆₃ for 1 h, 24.1% and 67.4% of *C. albicans* died, respectively. Scyampcin₄₄₋₆₃ at a dose of 6 μM killed 99.4% of *C. albicans* within 10 h, and 12 μM Scyampcin₄₄₋₆₃ killed 99.9% of *C. albicans* in 8 h (Fig. 2A). Exogenous ergosterol had less of an effect on Scyampcin₄₄₋₆₃ (MIC up to 2-fold) than amphotericin B (AMB) (MIC up to 8-fold) against *C. albicans* (Table S6). As Fig. S5 shown, the proportion of propidium iodide (PI) in *C. albicans* were decreased from 24.2% to 7.73%, 5.29%, and 4.98% when pretreated Scyampcin₄₄₋₆₃ with 100, 200, and 400 $\mu\text{g}/\text{mL}$ of ergosterol, respectively. Scyampcin₄₄₋₆₃ at a dose ≥ 6 μM significantly inhibited the biofilm formation of *C. albicans* (Fig. 2C), while ≥ 24 μM Scyampcin₄₄₋₆₃

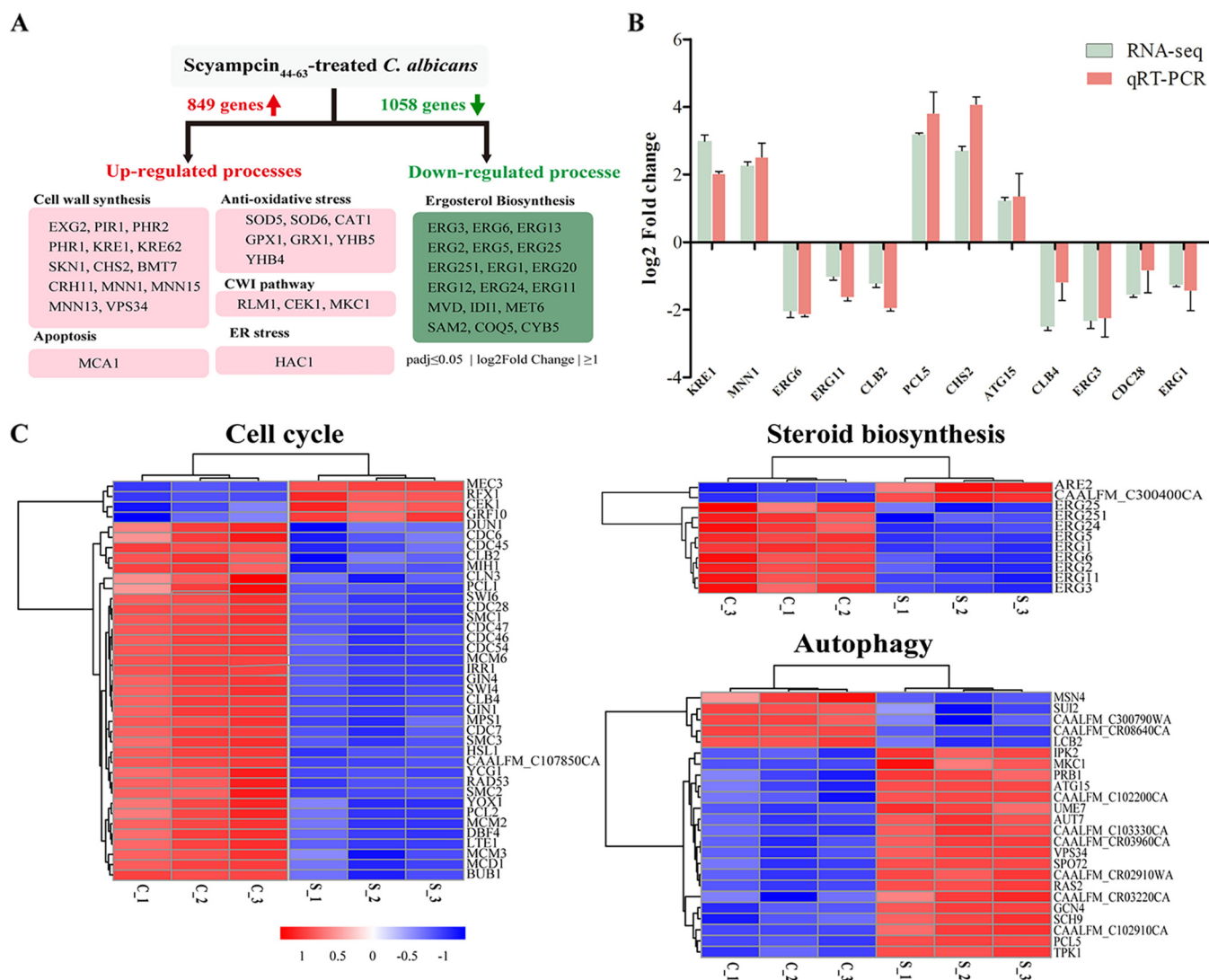


FIG 1 Transcriptomic analysis of Scyampcin₄₄₋₆₃-treated *C. albicans*. (A) Analysis of DEGs in *C. albicans* after Scyampcin₄₄₋₆₃ treatment. DEGs, differentially expressed genes. (B) Comparison of expression levels between RNA sequencing (RNA-seq) and quantitative reverse-transcription PCR (qRT-PCR). (C) Hierarchical clustering analysis of several enriched pathways. *C. albicans* cells were untreated or treated with Scyampcin₄₄₋₆₃ for 1 h, and RNA sequencing was performed. C₁, C₂, and C₃ represent three independent treatments of the control, and S₁, S₂, and S₃ represent three independent treatments of Scyampcin₄₄₋₆₃. Colored bars indicate the Z score, which was the normalized value of differential gene *FPKM*. The deeper red shades indicate higher expression levels, while the deeper blue shades indicate lower expression levels.

was effective against preformed biofilms of *C. albicans* (Fig. 2D). We further verified that Scyampcin₄₄₋₆₃ was also effective against hyphal forms of *C. albicans* (Fig. S3). The amphiphilic structure allows AMPs to interact with microbial membranes, causing membrane permeabilization, which is the most common microbicidal mechanism of AMPs. Thus, we used the fluorescent dyes SYTOX Green and PI/Syto 9 to evaluate the membrane permeability of *C. albicans* cells caused by Scyampcin₄₄₋₆₃. SYTOX Green and PI can cross the damaged membrane and excite green and red fluorescence after binding to nucleic acids, respectively. The fluorescence intensity of SYTOX Green in *C. albicans* was enhanced after exposed to different concentrations of Scyampcin₄₄₋₆₃ with concentration and time dependence (Fig. 2B). Scyampcin₄₄₋₆₃ promoted the uptake of PI by *C. albicans* and decreased the fluorescence intensity of Syto 9, indicating that the membrane of *C. albicans* was disrupted by Scyampcin₄₄₋₆₃ (Fig. 2E). In addition, the cells treated with Scyampcin₄₄₋₆₃ appeared smaller than those in the control group, and vacuolar expansion was observed (Fig. 2E). Furthermore, we confirmed this finding with flow cytometry. The forward scatter (FSC) was indeed decreased, which

TABLE 2 Significant enriched KEGG pathways of DEGs^a

ID	Description	Input no.	Background no.	Corrected P value
Upregulated				
cal01230	Biosynthesis of amino acids	29	107	1.39×10^{-5}
cal01210	2-Oxocarboxylic acid metabolism	13	32	1.64×10^{-4}
cal00220	Arginine biosynthesis	8	16	1.23×10^{-3}
cal00290	Valine, leucine, and isoleucine biosynthesis	7	13	1.23×10^{-3}
cal00340	Histidine metabolism	7	13	1.23×10^{-3}
cal04138	Autophagy: yeast	19	76	1.23×10^{-3}
cal01110	Biosynthesis of secondary metabolites	50	322	4.80×10^{-3}
cal00561	Glycerolipid metabolism	9	27	7.44×10^{-3}
cal00562	Inositol phosphate metabolism	7	22	3.10×10^{-2}
cal04136	Autophagy: other	7	22	3.10×10^{-2}
Downregulated				
cal03010	Ribosome	96	119	7.67×10^{-44}
cal03030	DNA replication	31	34	1.66×10^{-16}
cal03430	Mismatch repair	16	21	3.65×10^{-6}
cal03008	Ribosome biogenesis in eukaryotes	34	72	1.94×10^{-5}
cal03410	Base excision repair	13	18	9.60×10^{-5}
cal03440	Homologous recombination	13	20	4.66×10^{-4}
cal00230	Purine metabolism	24	52	7.38×10^{-4}
cal04111	Cell cycle: yeast	35	98	8.50×10^{-3}
cal03420	Nucleotide excision repair	16	38	3.09×10^{-2}
cal03020	RNA polymerase	13	29	3.43×10^{-2}
cal04113	Meiosis: yeast	30	89	3.88×10^{-2}
cal00100	Steroid biosynthesis	9	18	4.71×10^{-2}

^aThe corrected *p* values were adjusted using the Benjamini and Hochberg method, which helped to better control the false-positive rate of the multiple hypothesis test. DEG, differentially expressed gene.

indicated cell shrinkage. Cell shrinkage occurred prior to membrane permeabilization (Fig. S4). The aforementioned results evidently showed that Scyampcin₄₄₋₆₃ caused membrane permeabilization, inhibited the biofilm formation, and was effective against preformed biofilms of *C. albicans*.

Scyampcin₄₄₋₆₃ induces apoptosis in *C. albicans*. Transcriptomic analysis showed that Scyampcin₄₄₋₆₃ upregulated genes related to antioxidative stress and apoptosis, which indicated that Scyampcin₄₄₋₆₃ might cause oxidative damage and trigger apoptosis. We measured intracellular reactive oxygen species (ROS) levels by using an oxidant-sensitive dye, 2',7'-dichlorofluorescein diacetate (DCFH-DA), which turns into 2',7'-dichlorofluorescein (DCF) with strong fluorescence intensity after oxidation. In this study, the fluorescence intensity was significantly enhanced by Scyampcin₄₄₋₆₃ or H₂O₂, indicating the accumulation of ROS in *C. albicans* (Fig. 3A). Scyampcin₄₄₋₆₃ induced the generation of ROS in a concentration-dependent manner, while 10 mM H₂O₂ generated less ROS than 24 μM Scyampcin₄₄₋₆₃ at 2 h (Fig. 3A). ROS are mainly produced in mitochondria and cause damage to the mitochondrial membrane by dissipating its membrane potential (12). Thus, we used JC-1 to monitor the changes in mitochondrial membrane potential. In normal cells, JC-1 aggregates in the mitochondrial matrix and exhibits red fluorescence. When the mitochondrial membrane potential ($\Delta\Psi_m$) dissipates, JC-1 aggregates can be converted to JC-1 monomers (green fluorescence). After 2 h of treatment with 6 μM Scyampcin₄₄₋₆₃, some cells presented hyperpolarized mitochondrial membrane potential, while others completely lost mitochondrial membrane potential (Fig. 3B). Scyampcin₄₄₋₆₃ stimulated the generation of ROS and destroyed the mitochondrial membrane potential of *C. albicans*. Excessive ROS induce oxidative damage to important cellular components, such as proteins, lipids, or nucleic acids, and can trigger apoptosis (13). Furthermore, we used terminal deoxynucleotidyltransferase-mediated dUTP-biotin nick end labeling (TUNEL) staining to determine whether Scyampcin₄₄₋₆₃ induced apoptosis in *C. albicans*. Both 6 μM and

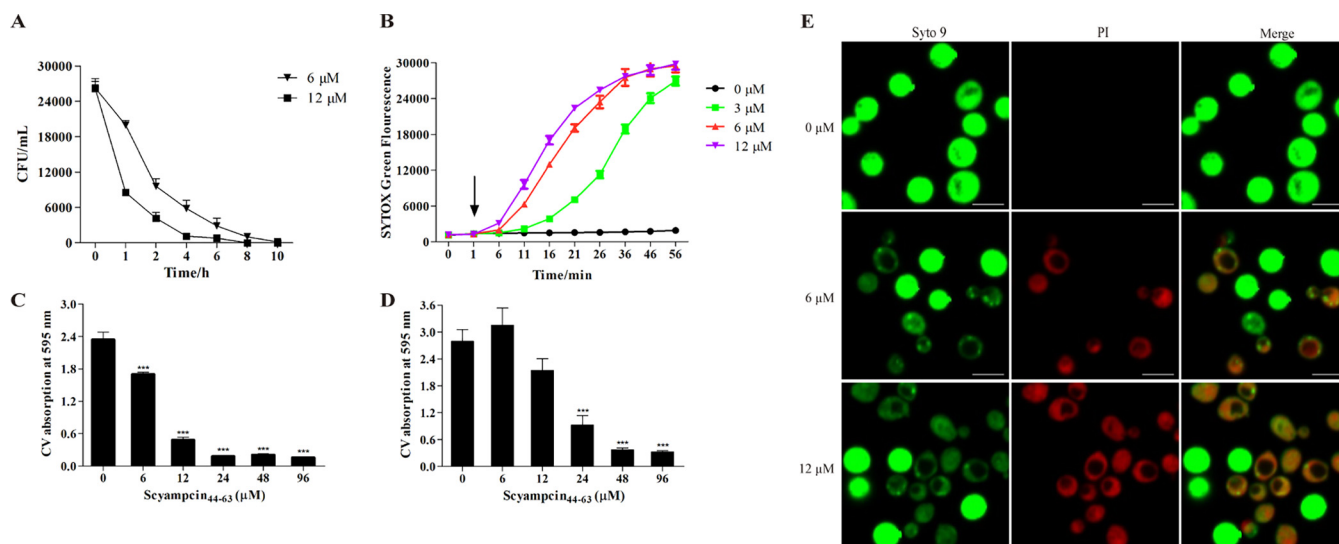


FIG 2 The candidacidal, anti-biofilm, and membrane permeability activities of Scyampcin₄₄₋₆₃. (A) Time-killing kinetics of Scyampcin₄₄₋₆₃ on *C. albicans*. (B) Scyampcin₄₄₋₆₃ enhanced SYTOX green fluorescence intensity. The arrow indicates the time of peptide addition. (C) Scyampcin₄₄₋₆₃ inhibited biofilm formation of *C. albicans*. (D) Scyampcin₄₄₋₆₃ was effective against preformed biofilm of *C. albicans*. (A to D) Representative results of three repeats are shown, and error bars represent standard errors of the means ($n = 3$). (E) Scyampcin₄₄₋₆₃ destroyed the membrane of *C. albicans*. *C. albicans* was exposed to Scyampcin₄₄₋₆₃ for 30 min and then stained with propidium iodide (PI)/Syto 9 for 15 min. The samples were imaged by confocal laser microscopy. The bars at the bottom right of each picture indicate 5 μ m. Asterisks indicate significant difference: *, $P < 0.05$; **, $P < 0.01$; ***, $P < 0.001$. Significant difference was compared with vehicle control (0 μ M in the images).

12 μ M Scyampcin₄₄₋₆₃ increased green fluorescence in *C. albicans*, indicating the occurrence of DNA fragmentation (Fig. 3C), which is a sign of apoptosis.

Scyampcin₄₄₋₆₃ induces cell cycle arrest at G₂/M phase. Several reports have shown that apoptosis is closely associated with cell cycle arrest, and the cell cycle of Scyampcin₄₄₋₆₃-treated *C. albicans* is one of the pathways significantly downregulated in KEGG enrichment analysis. Therefore, we detected the cell cycle of *C. albicans* after exposure to different concentrations of Scyampcin₄₄₋₆₃. Compared with the untreated group, after exposure to 3 μ M and 6 μ M Scyampcin₄₄₋₆₃, the proportions of G₂/M phase cells (from 24.08% to 68.25% and 74.19%, respectively) was increased, and both the G₁/G₀ phase (from 45.95% to 29.58% and 25.81%, respectively) and S phase proportions decreased (from 24.08% to 2.17% and 0.00%, respectively) (Fig. 4), indicating that the cell cycle of *C. albicans* was arrested at the G₂/M phase by Scyampcin₄₄₋₆₃.

Morphological change and extracellular DNA concentration. To explore the anti-candidal mechanism of Scyampcin₄₄₋₆₃, we used scanning electron microscopy (SEM) and transmission electron microscopy (TEM) to observe the morphological and ultrastructural changes of *C. albicans* induced by Scyampcin₄₄₋₆₃, respectively. The untreated yeasts were round, while the Scyampcin₄₄₋₆₃-treated yeasts were deformed and dented (Fig. 5A). TEM images showed that the cell wall was deformed, the membrane was dented and the vacuole was expanded in Scyampcin₄₄₋₆₃-treated yeasts. There were obvious organelle boundaries in the untreated yeasts, meanwhile, in the Scyampcin₄₄₋₆₃-treated yeasts, the organelles were barely visible (Fig. 5B). In addition, we measured the extracellular DNA concentration of *C. albicans* to check whether damaged nuclear and plasma membranes induced the leakage of DNA. The results showed that the concentrations of extracellular DNA in *C. albicans* were significantly elevated when exposed to 12 to 48 μ M Scyampcin₄₄₋₆₃ for 2 h and 4 h (Fig. 5C).

3-MA delayed the candidacidal effect of Scyampcin₄₄₋₆₃. We observed vacuolar expansion in *C. albicans* after treatment with Scyampcin₄₄₋₆₃ (Fig. 2E and 5B), and the autophagy pathway was one of the significantly upregulated pathways upon KEGG enrichment analysis (Table 2). Thus, we evaluated the effect of the autophagy inhibitor 3-methyladenine (3-MA) on the candidacidal activity of Scyampcin₄₄₋₆₃. 3-MA significantly delayed

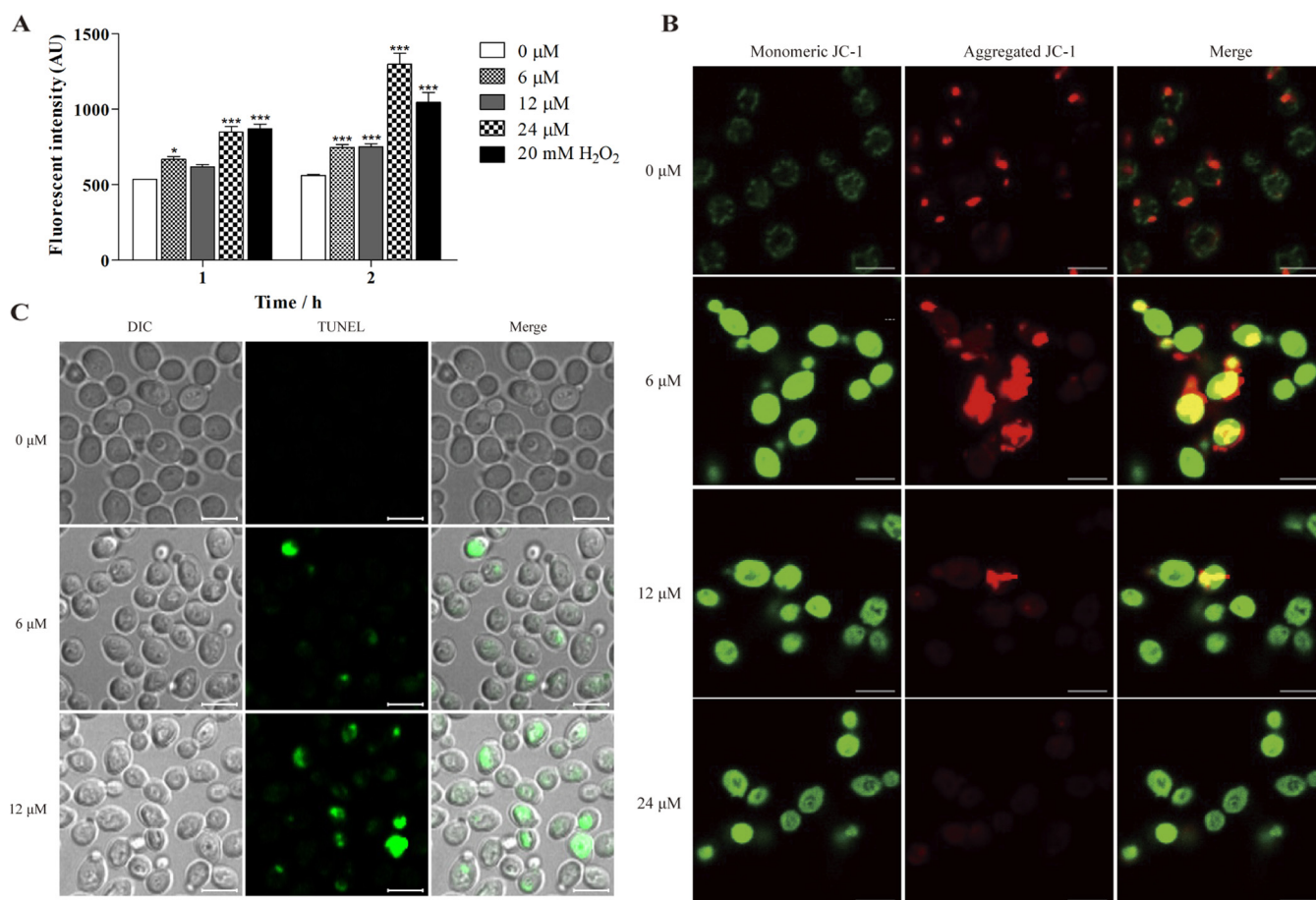


FIG 3 Scyampcin₄₄₋₆₃ triggered apoptosis of *C. albicans*. (A) Intracellular reactive oxygen species (ROS) levels. *C. albicans* cells (2.5×10^6 cells/mL) were pretreated with the 2',7'-dichlorofluorescein diacetate (DCFH-DA) probe for 30 min, and then the excessive stain was removed. The results were recorded with a multimode microplate reader (excitation/emission = 485 nm/525 nm) after incubation with Scyampcin₄₄₋₆₃ or H₂O₂ (as a positive control) for 1 and 2 h. Asterisks indicate significant difference: *, $P < 0.05$; **, $P < 0.01$; ***, $P < 0.001$, compared with control. Representative results of three repeats are shown, and error bars represent standard errors of the means ($n = 3$). (B) Scyampcin₄₄₋₆₃ destroyed $\Delta\Psi_m$. (C) DNA fragmentation caused by Scyampcin₄₄₋₆₃. Representative results of three repeats are shown. (B, C) *C. albicans* cells (2.5×10^6 cells/mL) exposed to Scyampcin₄₄₋₆₃ for 2 h. JC-1 and terminal deoxynucleotidyltransferase-mediated dUTP-biotin nick end labeling (TUNEL) staining were performed. The samples were observed by confocal laser microscopy. The bars on the bottom right of each picture indicate 5 μm . DIC, differential interference contrast.

the fungicidal rate of 3 μM Scyampcin₄₄₋₆₃ against *C. albicans* at 1 h and 2 h. 3-MA significantly decreased the candidacidal activity of 6 μM Scyampcin₄₄₋₆₃ at 30 min, 1 h, and 2 h. The remarkable influence of 3-MA on anti-candidal activity of 12 μM Scyampcin₄₄₋₆₃ occurred at 30 min and 1 h (Fig. 6).

Topical treatment with Scyampcin₄₄₋₆₃ decreased the fungal burden *in vivo*.

Because Scyampcin₄₄₋₆₃ possessed potent anti-candidal activity *in vitro*, we further evaluated the safety and antifungal effect of Scyampcin₄₄₋₆₃ in a murine model of VVC. Compared with the control (phosphate-buffered saline [PBS]) group, intravaginal treatment with Scyampcin₄₄₋₆₃ (12 μM and 48 μM) and fluconazole (100 $\mu\text{g}/\text{mL}$) did not cause any significant change in lactate dehydrogenase (LDH) levels, and both were relatively safe for mice (Fig. S6). Topical treatment with Scyampcin₄₄₋₆₃ or fluconazole significantly decreased the fungal burden in vaginal lavage fluid (Fig. 7A). The corresponding mean CFU levels were 1.67×10^5 for the PBS group and 6.5×10^3 , 3.4×10^3 , and 1.63×10^3 CFU/mL for the 12 μM Scyampcin₄₄₋₆₃, 48 μM Scyampcin₄₄₋₆₃, and 100 $\mu\text{g}/\text{mL}$ fluconazole treatment groups, representing 96.1%, 97.9%, and 99.9% inhibition of vaginal colonization, respectively. Consistent with the fungal burden results, fewer pseudohyphae were observed after treatment with Scyampcin₄₄₋₆₃ or fluconazole than in the PBS group (Fig. 7B).

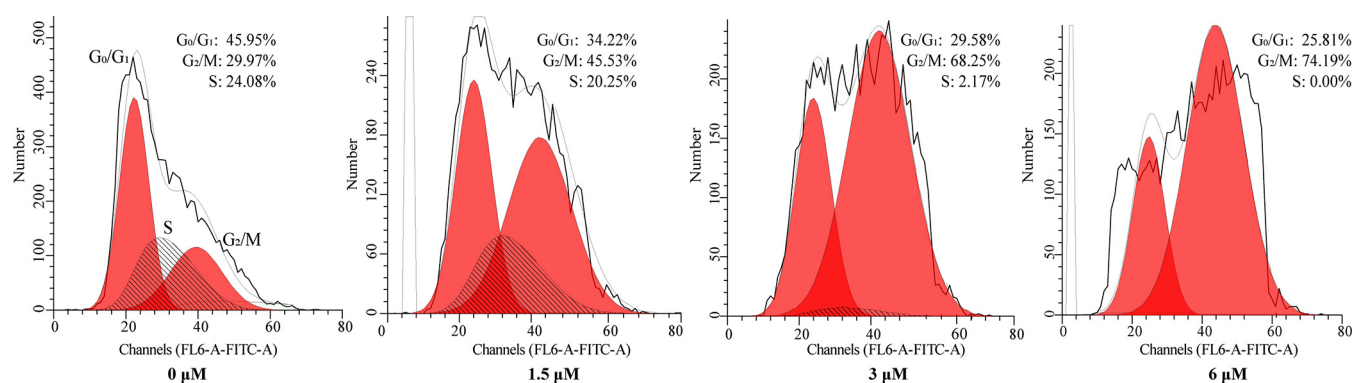


FIG 4 The effect of Scyampcin₄₄₋₆₃ on the cell cycle of *C. albicans*. *C. albicans* were collected after exposure to different concentrations of Scyampcin₄₄₋₆₃ and then fixed with precooled 70% ethanol. The fixed cells were washed with sodium citrate buffer twice, treated with RNase A for 1 h, and stained with SYTOX Green for 30 min. The DNA contents were measured with a flow cytometer. Representative results of three repeats are shown.

DISCUSSION

C. albicans is responsible for 90% of VVC cases, afflicting 75% of women globally (1). With the increasing incidence of azole-resistant and biofilm-forming *Candida* species, there is an urgent need to explore new antifungal drugs (3, 14). In the present study, we identified a novel AMP with broad-spectrum antimicrobial activity named Scyampcin₄₄₋₆₃ from the mud crab *S. paramamosain*. Scyampcin₄₄₋₆₃ inhibited *C. albicans* planktonic growth and biofilm formation and effectively inhibited preformed biofilms, without cytotoxicity toward mammalian cells (HaCaT and RAW264.7) or mouse erythrocytes. Thus, we performed RNA-seq to analyze the potential candidacidal mechanism of Scyampcin₄₄₋₆₃; the results suggest that Scyampcin₄₄₋₆₃ might inhibit ergosterol biosynthesis, trigger autophagic cell death and apoptosis, and interfere with the cell cycle. Following these clues, we designed experiments to verify the antifungal features and mechanism and further evaluated the efficacy of Scyampcin₄₄₋₆₃ *in vivo*.

Ergosterol is a vital component of the fungal plasma membrane that affects membrane permeability and the activity of membrane-bound enzymes and is also an important target for many antifungal drugs, such as azole and AMB (15). Consistent with the treatment with AMB (16) or MAF-1A (17), several ergosterol biosynthesis-related genes were downregulated in Scyampcin₄₄₋₆₃-treated *C. albicans*. We demonstrated that the plasma membrane permeability of *C. albicans* was constantly increasing in response to Scyampcin₄₄₋₆₃. Exogenous ergosterol decreased the activity of AMB or Scyampcin₄₄₋₆₃ against *C. albicans*, indicating that Scyampcin₄₄₋₆₃ might partially influence ergosterol biosynthesis and cause membrane damage in *C. albicans*.

Autophagy is an adaptation to cellular stress through engulfing damaged organelles and cytoplasmic components and degrading them within the lysosome/vacuole compartment (18). Excessive levels of autophagy contribute to autophagic cell death, which is accompanied by large-scale autophagic vacuolization in the cytoplasm (19). In the present study, the KEGG-enriched autophagy pathway of *C. albicans* was shown to be upregulated in response to Scyampcin₄₄₋₆₃. TEM images showed that untreated cells were round and that organelles were clearly presented in *C. albicans*, while Scyampcin₄₄₋₆₃-treated *C. albicans* cells exhibited deformed morphology, vacuolar expansion, and barely visible organelles. The autophagy inhibitor 3-MA significantly delayed the killing effect of Scyampcin₄₄₋₆₃ against *C. albicans*. Thus, we speculated that Scyampcin₄₄₋₆₃ caused organelle damage, resulting in the upregulation of autophagy-related genes and the induction of vacuolar expansion, which might ultimately trigger autophagic cell death in *C. albicans*. However, the underlying mechanism still needs further investigation.

Unlike autophagic cell death, intrinsic apoptosis has been widely demonstrated in *Candida* species (20). AMPs such as cecropin A (21) and psacothasin (22) induce apoptosis in *C. albicans*. Intrinsic apoptosis is accompanied by the accumulation of ROS and mitochondrial dysfunction. ROS are by-products of cellular metabolism (13). Excessive ROS

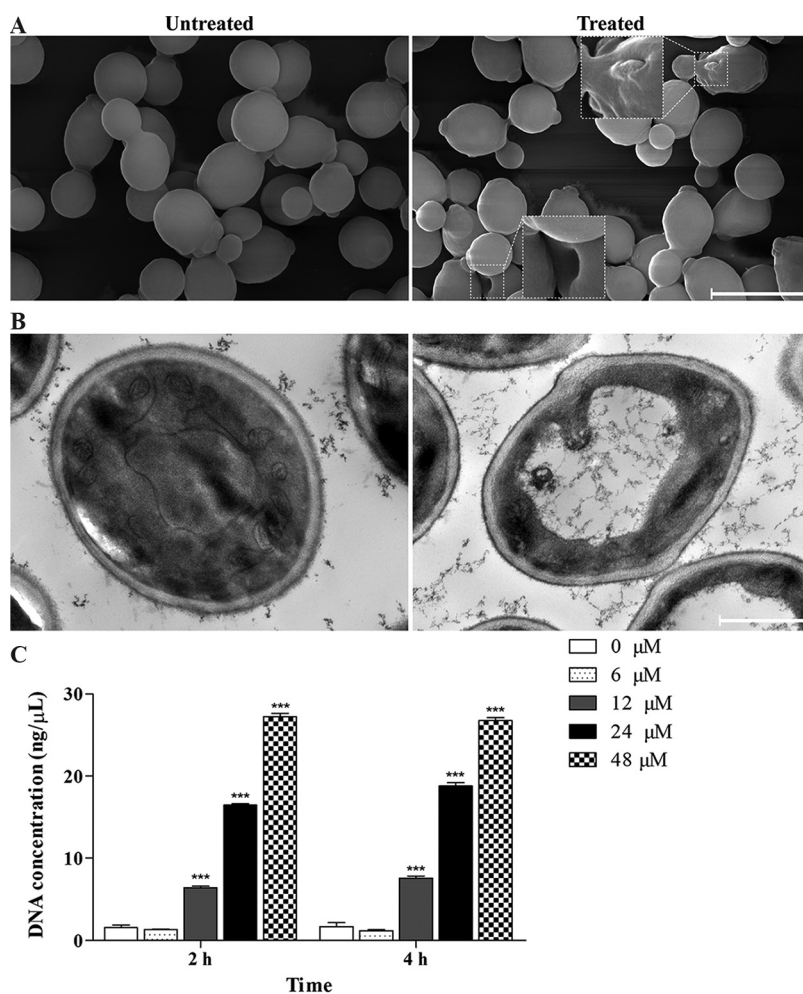


FIG 5 Morphological changes and extracellular DNA concentration of *C. albicans* induced by Scyampcin₄₄₋₆₃. (A, B) Morphological changes of *C. albicans* induced by Scyampcin₄₄₋₆₃. After incubation with 6 μM Scyampcin₄₄₋₆₃ for 1 h, the samples were subjected to SEM or TEM methods and photographed by scanning (A) and transmission (B) electron microscopy. The bars on the bottom right of the picture indicate 5 μm (A) and 1 μm (B). (A) Dotted boxes represent zoomed-in portions of samples. Representative results of three repeats are shown. (B) Representative images of two repeats. (C) Extracellular DNA concentration of *C. albicans* after treatment with Scyampcin₄₄₋₆₃. The supernatants of *C. albicans* were collected to detect the DNA concentration after exposure to Scyampcin₄₄₋₆₃. Representative results of three repeats are shown, and error bars represent standard errors of the means ($n = 3$). Asterisks indicate significant difference: *, $P < 0.05$; **, $P < 0.01$; ***, $P < 0.001$, compared with controls.

cause irreversible damage to proteins, lipids, nucleic acids, membranes, and organelles (22). Recently, many reported AMPs have been shown to induce cell death by generating ROS, such as plant defensins (NaD1, RsAFP2, HsAFP1, and PvD1) (22–27). Similarly, Scyampcin₄₄₋₆₃ significantly increased the intracellular ROS level in *C. albicans*. As mitochondria are both the source and target of intracellular ROS, and mitochondrial membrane potential is indispensable for maintaining mitochondrial functions, we used the JC-1 dye to demonstrate that Scyampcin₄₄₋₆₃ destroyed the mitochondrial membrane potential of *C. albicans*. Consistent with the process of hyperpolarization of the mitochondrial membrane potential induced by apoptotic agents (28), some cells presented hyperpolarization after exposure to 6 μM Scyampcin₄₄₋₆₃, which occurs before total loss of the mitochondrial membrane potential and cell death. Increased ROS and destroyed mitochondrial membrane potential are markers of apoptosis, and we further verified that Scyampcin₄₄₋₆₃ indeed triggered apoptosis by causing DNA fragmentation in *C. albicans*.

Several reports have shown that apoptosis is closely associated with cell cycle arrest; for example, antifungal natural products and their derivatives cause cellular apoptosis and

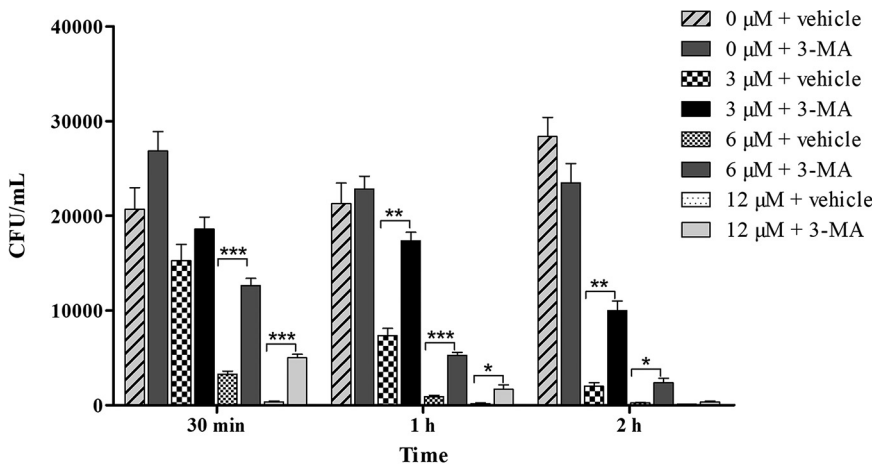


FIG 6 3-Methyladenine (3-MA) significantly delayed the candidacidal rate of Scyampcin₄₄₋₆₃. *C. albicans* was pretreated with or without 10 mM 3-MA for 1 h. Different concentrations of Scyampcin₄₄₋₆₃ were added and incubated for 30 min, 1 h, and 2 h. The mixed suspensions were diluted and spread onto yeast extract peptone dextrose agar plates ($n = 3$). Asterisks indicate significant difference: *, $P < 0.05$; **, $P < 0.01$; ***, $P < 0.001$. Significant differences were analyzed between the same concentration of Scyampcin₄₄₋₆₃ with and without (vehicle control) treatment with 3-MA. Representative results of two repeats are shown, and error bars represent standard errors of the means ($n = 3$).

dysregulate the cell cycle (29). The plant defensin HsAFP1 also causes *S. cerevisiae* cell cycle arrest at the G₂/M phase (30). AMB (4 to 8 μg/mL) (31) and an antifungal compound citral derivative (29) cause cell cycle arrest and apoptosis in *C. albicans*. The antimicrobial peptides APP and BUF (5–21) cause *C. albicans* cell cycle arrest in the S phase and subsequently inhibit normal processes (32). However, the precise link between the cell cycle and apoptosis in *C. albicans* remains unclear. In the present study, several cell cycle- and mitosis-related genes of *C. albicans* were downregulated after Scyampcin₄₄₋₆₃ treatment, and we demonstrated that Scyampcin₄₄₋₆₃ induced cell cycle arrest at the G₂/M phase in *C. albicans*,

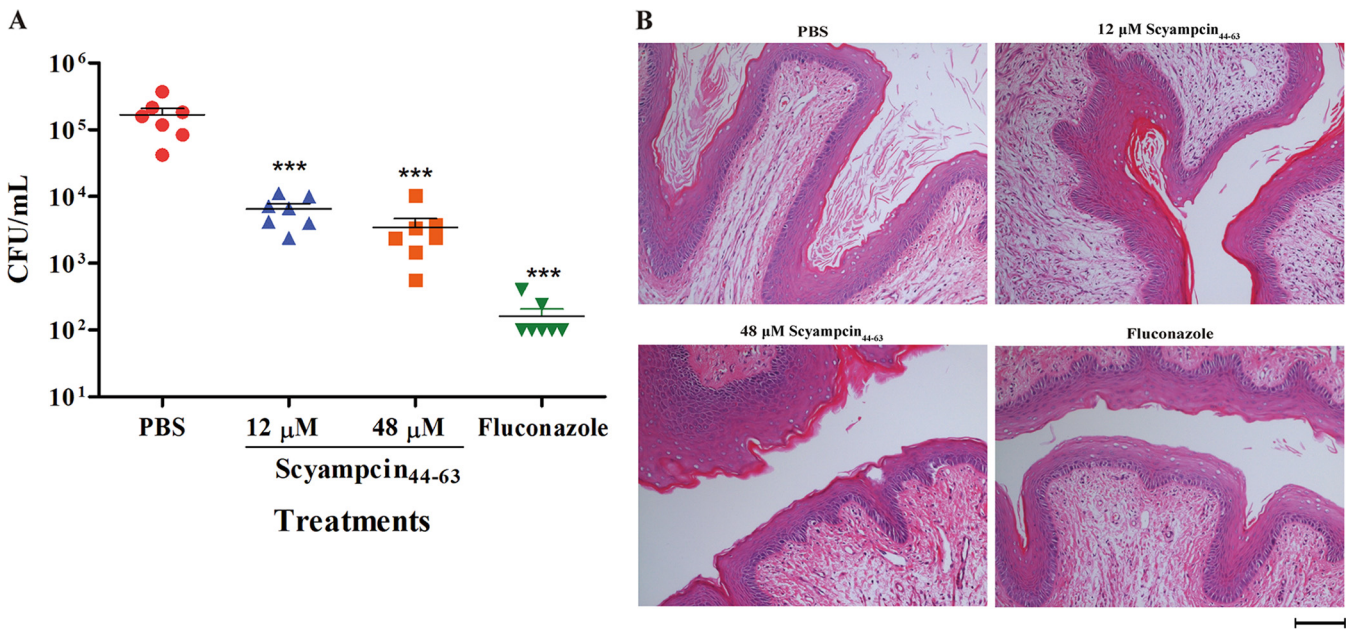


FIG 7 Efficacy of Scyampcin₄₄₋₆₃ as the topical treatment for murine vulvovaginal candidiasis (VVC). (A) The fungal burden in vaginal lavage fluid. Representative results of two repeats are shown, and error bars represent standard errors of the means ($n = 7$), *** indicates $P < 0.001$. (B) Histological analysis of vaginal tissues with hematoxylin and eosin (HE) staining. The bar at the bottom right of the picture indicates 100 μm. Each group of mice ($n = 7$) continuously received treatment with phosphate-buffered saline (PBS), 12 μM Scyampcin₄₄₋₆₃, 48 μM Scyampcin₄₄₋₆₃, or 100 μg/mL fluconazole for 3 days (at intervals of 12 h) 24 h postinfection.

suggesting that one of the candidacidal mechanisms of Scyampcin₄₄₋₆₃ is interference with cell proliferation and division.

The murine model of VVC has been well established, and it is helpful to evaluate the efficacy of antifungal agents, which is an indispensable step for future applications. Cytokines, antibodies, probiotics, and AMPs play vital roles in the immune defense of vaginal tissues against the invasion of *Candida* species (33). Several AMPs, such as gomesin (34), Hst-5 (35), and NFAP2 (3) significantly reduce the number of *C. albicans* cells in a murine model of VVC, even though the vaginal fungal burden is still present. Similarly, in this study, intravaginal administration of Scyampcin₄₄₋₆₃ was effective in reducing the number of *C. albicans* cells, and fewer pseudohyphae were observed in the murine vagina, which could not eliminate the vaginal fungal burden to undetectable levels. Although AMPs are considered promising new antibiotic candidates, there are still some issues (low stability and bioavailability, potential toxicity, and high cost) that need to be solved for their application in the clinic (36). Some AMPs (such as LL-37 and β -defensins) are severely dysfunctional under physiological salt concentrations and are affected by host factors (37). These findings may partially explain why AMPs cannot fully eradicate the vaginal fungal burden in the murine model of VVC. Furthermore, *C. albicans* is a polymorphic fungus that grows as yeast, pseudohyphae, and true hyphae (38). *C. albicans* has the chance to convert yeast to hyphae once in contact with host cells, and the hyphae are more resistant to antifungal drugs, which greatly hampers treatment *in vivo* (39). Seeking methods to improve antimicrobial activity and safety *in vivo* requires further research. Previous studies have shown that some AMPs act synergistically with AMPs, surface-active agents, and traditional antibiotics, and these synergistic effects enhance their antimicrobial effect (36). For example, NFAP2 combined with fluconazole indeed enhances the efficacy *in vivo* (3). Loading AMPs into systems based on nanoparticles or micro-particles with a targeted delivery capacity is another strategy to overcome the shortcomings of AMPs (36). In the present study, we provide an option for topical treatment of murine VVC with Scyampcin₄₄₋₆₃, which needs further optimization. In the future, we will attempt to explore the synergistic effect of Scyampcin₄₄₋₆₃ with AMPs or antibiotics and optimize the delivery approach to improve the efficacy of AMP *in vivo*.

MATERIALS AND METHODS

Scyampcin gene cloning. The full-length cDNA of Scyampcin was amplified by rapid amplification of cDNA ends (RACE) PCR. The primers for RACE PCR were listed in Table S1. Mud crabs (*S. paramamosain*, weight: 300 ± 10 g) were obtained from Zhangpu FishFarm (Fujian, China), and tissues or organs were collected for further RNA extraction, respectively. TRIzol reagent (Invitrogen, USA), PrimeScript RT reagent kit with a genomic DNA (gDNA) eraser kit (TaKaRa, China), SMARTer RACE 5'/3' kit were used to extract total RNA, synthesize cDNA, and RACE cDNA, respectively. The obtained fragment was cloned into pMD18-T Vector (TaKaRa, China) and sequenced by Bioray Biotechnology (Xiamen, China).

Bioinformatics analysis and synthesis of Scyampcin₄₄₋₆₃. The homology and similarity of Scyampcin were analyzed at the National Center for Biotechnology Information (NCBI). The ORF was predicted by the orfinder tool of NCBI. The pI/M_w was computed by the ExPASy tool. PSIPRED 4.0 and I-TASSER were used to predict secondary and tertiary structure, respectively. CAMP_{R3} was used to predict antimicrobial region within peptides. The aforementioned database or analysis software-related websites are listed in Table S2. Scyampcin₄₄₋₆₃ (GKKKKRNMMKTKEPGIIFFF-NH₂) was chemically synthesized by Genscript (Nanjing, China). The purity ($\geq 95\%$) and molecular weight of both preparations were further confirmed by high performance liquid chromatography (HPLC) and mass spectrometry. The powdered peptide was stored at -80°C until use. The peptide was dissolved in sterile water and stored at -20°C .

Strains and cultivation. The strains used in antimicrobial activity assay were purchased from the China General Microbiological Culture Collection Center (CGMCC). Bacterial strains were cultivated in nutrient broth (NB) at 37°C , and fungal strains were cultured in yeast extract peptone dextrose (YPD) or potato dextrose agar (PDA) at 28°C . All experiments were strictly executed according to the guidelines of the standard biosecurity and institutional safety procedures established by Xiamen University.

Cell line and cultivation. Murine macrophage RAW264.7 was cultured in Dulbecco's minimal essential medium (DMEM) containing 10% fetal bovine serum (FBS). Human immortalized keratinocytes HaCaT were maintained in minimal essential medium (MEM) with 10% FBS. The aforementioned cell lines were cultivated at 37°C with 5% CO_2 atmosphere.

Cytotoxicity assay. The CellTiter 96 AQ_{UEOUS} assay (Promega, USA) was used to determine cell viability (8). The CellTiter 96 AQ_{UEOUS} Assay is composed of 3-(4,5-dimethylthiazol-2-yl)-5-(3-carboxymethoxyphenyl)-2-(4-sulfophenyl)-2H-tetrazolium (MTS) and phenazine methosulfate (PMS). RAW264.7 or HaCaT were seeded to 96-well plates (1×10^4 cells/well) for 18 to 24 h. Fresh media with or without different concentrations of the test peptide were added slightly to the wells and incubated for another 24 h. The vehicle group was

treated with fresh medium containing 5% water. After incubation with tested peptide, 20 μ L of MTS-PMS reagent was added to each well and incubated for 1 to 4 h. The absorbance of each well was measured at 492 nm in a multimode microplate reader (Tecan, Switzerland). The experiments were repeated three times independently.

Hemolytic activity assay. The hemolytic activity of Scyampcin₄₄₋₆₃ on mouse erythrocytes was measured as previously reported (40). Briefly, the erythrocytes were collected after washed three times with saline, resuspended in saline, and adjusted to 4% erythrocytes. The erythrocytes were incubated with different concentrations of Scyampcin₄₄₋₆₃ for 1 h at 37°C. Treatment of saline (containing 5% water, as a vehicle control) and 1% Triton X-100 were used as negative and positive controls, respectively. The supernatants were centrifuged, their absorbance at 540 nm was measured using a multimode microplate reader (Tecan, Switzerland), and the ratio of hemolysis was calculated as previously described (40). The experiments were repeated three times independently.

Antimicrobial activity assay. The broth dilution method was used to determine the antimicrobial activity of the peptide based on a previous report with some modifications (9). Briefly, microorganisms were cultured to midlogarithmic phase and then harvested. The bacteria were diluted to approximately 5×10^5 CFU/mL with Mueller-Hinton broth, and yeasts or conidia of filamentous fungi were diluted to approximately 5×10^4 cells/mL in RPMI 1640 medium buffered with 0.165 mol/liter 3-morpholinopropane-1-sulfonic acid (pH of 7.0, referred to as RPMI-MOPS). Finally, the obtained microbial suspensions were mixed with serially diluted peptides in 96-well plates and then incubated under the corresponding conditions for 24 or 48 h. The final concentration contains 50% RPMI-MOPS (vehicle control). The MIC, MBC, and MFC values were recorded as previously described (9). The experiments were performed three times independently.

The effect of exogenous ergosterol on the MICs of Scyampcin₄₄₋₆₃ or amphotericin B (AMB) was determined according to the aforementioned antimicrobial activity assay, but 50, 100, or 200 μ g/mL ergosterol was added to RPMI-MOPS (Sigma-Aldrich, USA) (24). The experiments were repeated three times independently.

Transcriptomic analysis. *C. albicans* (3.75×10^7 cells/mL in RPMI-MOPS) were incubated with an equal volume of Scyampcin₄₄₋₆₃ maintained in shaking at 28°C for 1 h. The yeast cells were collected and ground in liquid nitrogen. Total RNA was extracted with TRIzol reagent. RNA integrity was assessed, and qualified RNA was used to construct a library. Transcriptomic sequencing was performed by Novogene Corporation (Beijing, China) using the Illumine NovaSeq platform. The reference genome and annotation files of *C. albicans* SC5314 were downloaded from NCBI (RefSeq accession number [GCF_000182965.3](https://www.ncbi.nlm.nih.gov/RefSeq/annotation/ accession/GCF_000182965.3)). Hisat2 version 2.0.5 was applied to construct an index of the reference genome, and sequence alignment was performed between paired-end clean reads and the reference genome. The reads mapped to each gene were counted using FeatureCounts version 1.5.0-p3. The DESeq2 R package (1.20.0) was used to analyze differential gene expression, with thresholds of corrected *P* values < 0.05 and $|\log_2(\text{fold change})| > 1$ (*P* values were corrected based on Benjamini and Hochberg's approach). Kyoto Encyclopedia of Genes and Genomes (KEGG) enrichment analysis of DEGs was performed using the clusterProfiler R package (3.4.4).

Time-killing kinetics. Time-killing kinetics of different concentrations of peptide were conducted in the same way as the antimicrobial activity assay. The cell density of *C. albicans* was adjusted to approximately 5×10^4 cells/mL. The suspensions of *C. albicans* were mixed with equal volumes of testing peptide ($1 \times$, $2 \times$ MBC) and incubated for 0, 1, 2, 4, 6, 8, or 10 h. The mixed suspensions were diluted and spread onto yeast extract peptone dextrose agar plates. After incubation for 24 h, the surviving colonies were counted. The experiments were repeated three times independently. When evaluating the effect of 3-MA on the candidacidal activity of Scyampcin₄₄₋₆₃, *C. albicans* cells were pretreated with or without 10 mM 3-MA for 1 h. Different concentrations of Scyampcin₄₄₋₆₃ were added and incubated for 30 min, 1 h, and 2 h. The final concentration contains 50% RPMI-MOPS (vehicle control). The mixed suspensions were diluted and spread onto plates. After incubation for 24 h, the surviving colonies were counted. The experiments were repeated twice independently.

Antibiofilm activity assay. Antibiofilm activity assay was performed as described previously, with some modifications (41). Briefly, 200 μ L of a 2.5×10^6 CFU/mL suspension of *C. albicans* in RPMI-MOPS was seeded in 96-well plates for 4 or 24 h, followed by washing with RPMI-MOPS to remove planktonic *C. albicans*. Fresh RPMI-MOPS with or without Scyampcin₄₄₋₆₃ was added to the plate and further incubated for 24 h. The final concentration contains 50% RPMI-MOPS (vehicle control). After incubation, the planktonic *C. albicans* were removed by washing three times with sterile water. The biofilm was then stained with 100 μ L of 0.1% crystal violet. Excessive stains were removed by washing the plate three times, 95% ethanol was used to dissolve the stain, and the absorbance was measured at 595 nm. The experiments were repeated three times independently.

Evaluation of plasma membrane permeabilization. A SYTOX Green nucleic acid stain (Invitrogen, USA) and LIVE/DEAD FungaLight yeast viability kit (Invitrogen, USA) were used to measure the cell membrane permeabilization induced by Scyampcin₄₄₋₆₃. SYTOX Green is impermeable to intact membranes and exhibits more than 500-fold fluorescence enhancement after crossing compromised membranes and binding nucleic acids. *C. albicans* (2.5×10^6 CFU/mL) was suspended in Hanks' balanced salt solution (HBSS) containing 5 μ M SYTOX Green, and an equal volume of Scyampcin₄₄₋₆₃ at different concentrations was added to each well. The final concentration contains 50% HBSS (vehicle control). The fluorescence intensities (excitation [Ex], 485 nm; emission [Em], 525 nm) were constantly recorded every 5 min with a multimode microplate reader (Tecan, Switzerland). The experiments were repeated three times independently. The LIVE/DEAD FungaLight yeast viability kit contains 3.34 mM SYTO 9 green-fluorescent and 20 mM PI red-fluorescent nucleic acid stain. Syto 9 staining labels all yeast cells with intact or damaged membranes, while PI penetrates only yeast cells with damaged membranes, resulting in a

reduced fluorescence intensity of Syto 9. A 2.5×10^6 CFU/mL *C. albicans* suspension in RPMI-MOPS was exposed to an equal volume of Scyampcin₄₄₋₆₃ for 30 min. The final concentration contains 50% RPMI-MOPS (vehicle control). The samples were washed twice and suspended in HBSS containing Syto 9 and PI dye. The samples were transferred to poly-L-lysine slides and further stained for 15 min. Finally, the samples were imaged by confocal laser scanning microscopy (Zeiss, Germany). The experiments were repeated three times independently.

Measurement of intracellular ROS. Intracellular ROS were measured by using the cell-permeant reagent DCFH-DA (13). Once DCFH-DA enters the cell, DCFH-DA is hydrolyzed by cytoesterase to form DCFH, which is then rapidly oxidized to produce the strongly fluorescent product DCF. Briefly, fungal cells were pre-treated with a DCFH-DA (Tocris Bioscience, UK) probe for 30 min at 28°C. After incubation, excessive probes were removed by washing twice with sterile PBS. Then, the fungi were resuspended in fresh RPMI-MOPS with or without different concentrations of Scyampcin₄₄₋₆₃ or H₂O₂. The final concentration contains 50% RPMI-MOPS (vehicle control). The fluorescence intensities (Ex/Em = 485 nm/525 nm) were recorded using a multi-mode microplate reader (Tecan, Switzerland). The experiments were repeated three times independently.

Mitochondrial membrane potential ($\Delta\Psi_m$). The effect of Scyampcin₄₄₋₆₃ on the $\Delta\Psi_m$ of *C. albicans* was determined with the lipophilic cationic dye JC-1 (5,5',6,6'-tetrachloro-1,1',3,3'-tetraethylimida-carbocyanine iodide, Solarbio) (42). Briefly, *C. albicans* (2.5×10^6 cells/mL) in RPMI-MOPS were exposed to different concentrations of Scyampcin₄₄₋₆₃ for 2 h at 28°C. The final concentration contains 50% RPMI-MOPS (vehicle control). After incubation, the suspensions were washed and stained with JC-1 at 37°C for 15 min. The excessive stains were washed off, and the samples were photographed on a confocal laser microscope (Zeiss, Germany). The experiments were repeated three times independently.

TUNEL assay. Apoptosis in *C. albicans* was detected by terminal deoxynucleotidyl transferase dUTP nick end labeling (TUNEL) assays as previously reported with some modifications (9). Briefly, *C. albicans* (2.5×10^6 cells/mL) in RPMI-MOPS were treated with or without Scyampcin₄₄₋₆₃ for 2 h at 28°C. The final concentration contains 50% RPMI-MOPS (vehicle control). The samples were washed twice with PBS and then fixed in 4% paraformaldehyde for more than 30 min at 4°C. The traces of paraformaldehyde were washed with PBS, and the cells were permeabilized with 0.3% Triton X-100 on ice for 30 min. TUNEL staining was performed according to the manufacturer's instructions of the one-step TUNEL apoptosis assay kit (Beyotime, China). After staining, the samples were imaged with a confocal laser microscope. The experiments were repeated three times independently.

Scanning electron microscopy (SEM). SEM was applied to observe morphological changes in *C. albicans* caused by Scyampcin₄₄₋₆₃. The final concentration contains 50% RPMI-MOPS (vehicle control). After incubation, fungal cells were fixed with 2.5% glutaraldehyde at 4°C for more than 90 min and washed three times before adhering to the surface of poly-L-lysine-coated glass slides. After 1 h of adhesion, the samples were dehydrated in graded ethanol (30% ethanol for 5 min, 50% ethanol for 5 min, and 70% ethanol for 10 min, where the above steps were performed on ice; and then 80% ethanol for 10 min, 95% ethanol for 15 min, and 100% ethanol twice for 15 min). Then all samples were critical point dried, coated with gold particles, and photographed with a field emission scanning electron microscope (FEI Quanta 650 FEG, USA). The experiments were repeated three times independently.

Transmission electron microscopy (TEM). TEM samples were prepared following the protocol reported by Liu and colleagues (43) with some modifications. Briefly, *C. albicans* (1.25×10^7 cells/mL) were suspended in RPMI-MOPS, and an equal volume of peptide or sterile water (vehicle control) was added and followed by incubated for 1 h (28°C, 230 rpm). After treatment, the fungal cells were fixed with 2.5% glutaraldehyde and 0.5% paraformaldehyde. Glutaraldehyde and paraformaldehyde were diluted in 0.2 M phosphate buffer (pH of 6.8) and PIPES buffer (pH of 6.8), respectively. PIPES buffer contained 1 mM MgCl₂, 1 mM CaCl₂, and 0.1 M sorbitol. After fixation for 2 h at 4°C, the fungal cells were washed three times and pre-embedded in 2% agar. Then the specimens were postfixed with 1.5% KMnO₄ for 2 h at 4°C and washed three times with sterile water. All samples were dehydrated in a graded acetone series (50%, 70%, 85%, 95%, 100%, 100%, and 100%) for 5 min each. After dehydration, all samples were transferred to graded ratios between epoxy resin and acetone (1:3, 1:1, and 3:1) for 1.5 h each, and all samples were incubated in pure epoxy resin overnight. Finally, all samples were sectioned into ultrathin sections, stained with uranyl acetate and lead citrate, and observed under a transmission electron microscope (Hitachi HT-7800, Japan). The experiments were repeated two times independently.

Measurement of extracellular DNA concentration. *C. albicans* (2.5×10^8 cells/mL) in RPMI-MOPS were exposed to different concentrations of peptide or sterile water (vehicle control) and incubated for 2 h or 4 h. After incubation, the centrifuged supernatants were collected and measured using a NanoDrop 2000 spectrophotometer (Thermo Fisher Scientific, USA). The experiments were repeated three times independently.

Cell cycle assay. The DNA-specific fluorescent dye Sytox Green was applied to measure the DNA content. *C. albicans* (10^6 cells) were collected after exposure to different concentrations of Scyampcin₄₄₋₆₃ for 1 h. The final concentration contains 50% RPMI-MOPS (vehicle control). The samples were washed twice with 50 mM sodium citrate buffer and then fixed in cold 70% ethanol at 4°C for 12 h. The washing process was repeated for twice, and the cells were resuspended in buffer containing RNase A and incubated for 1 h at 37°C. SYTOX Green was then added and stained for 30 min (44). The DNA contents were measured with flow cytometer (Becton, Dickinson, USA). The data were analyzed using ModFit LT software (Verity Software House, USA). The experiments were repeated three times independently.

Murine model of VVC. Healthy C57BL/6J female mice (6 to 8 weeks old, 16 to 18 g) were purchased from GemPharmatech and acclimated for 1 week before the experiment. The mice were housed in individually ventilated cages (IVCs) on a 12-h light:12-h dark cycle at room temperature and provided access to sterile food and water *ad libitum*. The murine model of *Candida* vaginitis was constructed following a

previously described study with some modifications (35, 45). Briefly, each mouse was injected subcutaneously with 100 μL of sesame oil containing 200 μg of estradiol valerate (Sigma-Aldrich, United States). Three days later, each mouse was inoculated intravaginally with 10 μL of *C. albicans* (2.5×10^7 CFU/mL). Twenty-four hours postinfection, mice received vaginal perfusion of 10 μL phosphate-buffered saline or different concentrations of Scyampcin₄₄₋₆₃ (12 or 48 μM /group) or 100 $\mu\text{g}/\text{mL}$ fluconazole every 12 h. After 3 consecutive days, the vagina of each mouse was rinsed with 200 μL of PBS. The lavage fluid was diluted with PBS and then spread on Sabouraud's dextrose agar plates containing 1.25 $\mu\text{g}/\text{mL}$ chloramphenicol (Solarbio, China) for fungal quantification. The aforementioned animal experiments were performed according to national guidelines and approved by the Laboratory Animal Management and Ethics Committee of Xiamen University (XMULAC20220048). The experiments were performed twice independently.

For histology, the vaginal tissues were fixed with 4% formaldehyde, and then paraffin-embedded vaginal tissues were obtained. Sections were cut from the embedded tissues and subjected to hematoxylin and eosin staining (3).

Statistical analysis. All data are represented as the means \pm standard error of the mean. Two-tailed Student's *t* test, one-way analysis of variance (ANOVA) or two-way ANOVA was used to analyze the differences between different groups. Figure 2 and 7 used one-way ANOVA, Fig. 3 used two-way ANOVA, and the other figures used Student's *t* test. *P* values < 0.05 were considered significant.

The DESeq2 R package (1.20.0) was used to analyze transcriptomic data for differential gene expression with thresholds of corrected *P* values < 0.05 and $|\log_2(\text{fold change})| > 1$ (*P* values corrected base on Benjamini and Hochberg's approach).

Data availability. All relevant data are within the article and its supporting information files. The full-length cDNA sequence of Scyampcin and transcriptomic data of *C. albicans* are both available on NCBI database (GenBank accession number [MW388710](#); BioProject number [PRJNA906206](#)).

SUPPLEMENTAL MATERIAL

Supplemental material is available online only.

SUPPLEMENTAL FILE 1, DOCX file, 11.1 MB.

ACKNOWLEDGMENTS

We appreciate laboratory engineers Huiyun Chen, Zhiyong Lin, and Hui Peng providing technical assistance.

This study was supported by grant U1805233/41806162 from the National Natural Science Foundation of China, grant 2021J05008 from the Natural Science Foundation of Fujian Province, China, grant FJHY-YYKJ-2022-1-14 from Fujian Ocean and Fisheries Bureau, and grant 22CZP002HJ08 from the Xiamen Ocean and Fishery Development Special Fund Project through the Xiamen Municipal Bureau of Ocean Development.

REFERENCES

- Willems HME, Ahmed SS, Liu J, Xu Z, Peters BM. 2020. Vulvovaginal candidiasis: a current understanding and burning questions. *J Fungi* 6:27. <https://doi.org/10.3390/jof6010027>.
- Sobel JD. 2007. Vulvovaginal candidosis. *Lancet* 369:1961–1971. [https://doi.org/10.1016/S0140-6736\(07\)60917-9](https://doi.org/10.1016/S0140-6736(07)60917-9).
- Kovács R, Holzknrecht J, Hargitai Z, Papp C, Farkas A, Borics A, Tóth L, Váradi G, Tóth GK, Kovács I, Dubrac S, Majoros L, Marx F, Galgóczy L. 2019. *In vivo* applicability of *Neosartorya fischeri* antifungal protein 2 (NFAP2) in treatment of vulvovaginal candidiasis. *Antimicrob Agents Chemother* 63:e01777-18. <https://doi.org/10.1128/AAC.01777-18>.
- Ng SMS, Yap YYA, Cheong JWD, Ng FM, Lau QY, Barkham T, Teo JWP, Hill J, Chia CSB. 2017. Antifungal peptides: a potential new class of antifungals for treating vulvovaginal candidiasis caused by fluconazole-resistant *Candida albicans*. *J Pept Sci* 23:215–221. <https://doi.org/10.1002/psc.2970>.
- Struyfs C, Cammue BPA, Thevissen K. 2021. Membrane-interacting antifungal peptides. *Front Cell Dev Biol* 9:649875. <https://doi.org/10.3389/fcell.2021.649875>.
- Brogden KA. 2005. Antimicrobial peptides: pore formers or metabolic inhibitors in bacteria? *Nat Rev Microbiol* 3:238–250. <https://doi.org/10.1038/nrmicro1098>.
- Huang WS, Wang KJ, Yang M, Cai JJ, Li SJ, Wang GZ. 2006. Purification and part characterization of a novel antibacterial protein Scygonadin, isolated from the seminal plasma of mud crab, *Scylla serrata* (Forsk., 1775). *J Exp Mar Biol Ecol* 339:37–42. <https://doi.org/10.1016/j.jembe.2006.06.029>.
- Yang Y, Chen FY, Chen HY, Peng H, Hao H, Wang KJ. 2020. A novel antimicrobial peptide scyeproc from mud crab *Scylla paramamosain* showing potent antifungal and anti-biofilm activity. *Front Microbiol* 11:1589. <https://doi.org/10.3389/fmicb.2020.01589>.
- Chen YC, Yang Y, Zhang C, Chen HY, Chen F, Wang KJ. 2021. A novel antimicrobial peptide Spamosin₂₆₋₅₄ from the mud crab *Scylla paramamosain* showing potent antifungal activity against *Cryptococcus neoformans*. *Front Microbiol* 12:746006. <https://doi.org/10.3389/fmicb.2021.746006>.
- Zhu X, Chen F, Li S, Peng H, Wang KJ. 2021. A novel antimicrobial peptide sparanegtin identified in *Scylla paramamosain* showing antimicrobial activity and immunoprotective role *In vitro* and *in vivo*. *Int J Mol Sci* 23:15. <https://doi.org/10.3390/ijms23010015>.
- Jiang M, Chen R, Zhang J, Chen F, Wang KJ. 2022. A novel antimicrobial peptide Spampcin₅₆₋₈₆ from *Scylla paramamosain* exerting rapid bactericidal and anti-biofilm activity *in vitro* and anti-infection *in vivo*. *Int J Mol Sci* 23:13316. <https://doi.org/10.3390/ijms232113316>.
- Simon HU, Haj-Yehia A, Levi-Schaffer F. 2000. Role of reactive oxygen species (ROS) in apoptosis induction. *Apoptosis* 5:415–418. <https://doi.org/10.1023/a:1009616228304>.
- Thannickal VJ, Fanburg BL. 2000. Reactive oxygen species in cell signaling. *Am J Physiol Lung Cell Mol Physiol* 279:L1005-28. <https://doi.org/10.1152/ajplung.2000.279.6.L1005>.
- Perlin DS, Rautemaa-Richardson R, Alastruey-Izquierdo A. 2017. The global problem of antifungal resistance: prevalence, mechanisms, and management. *Lancet Infect Dis* 17:e383–e392. [https://doi.org/10.1016/S1473-3099\(17\)30316-X](https://doi.org/10.1016/S1473-3099(17)30316-X).
- De Backer MD, Ilyina T, Ma XJ, Vandoninck S, Luyten WH, Vanden Bossche H. 2001. Genomic profiling of the response of *Candida albicans* to itraconazole

- treatment using a DNA microarray. *Antimicrob Agents Chemother* 45: 1660–1670. <https://doi.org/10.1128/AAC.45.6.1660-1670.2001>.
16. Liu TT, Lee REB, Barker KS, Lee RE, Wei L, Homayouni R, Rogers PD. 2005. Genome-wide expression profiling of the response to azole, polyene, echinocandin, and pyrimidine antifungal agents in *Candida albicans*. *Antimicrob Agents Chemother* 49:2226–2236. <https://doi.org/10.1128/AAC.49.6.2226-2236.2005>.
 17. Wang T, Xiu J, Zhang Y, Wu J, Ma X, Wang Y, Guo G, Shang X. 2017. Transcriptional responses of *Candida albicans* to antimicrobial peptide MAF-1A. *Front Microbiol* 8:894. <https://doi.org/10.3389/fmicb.2017.00894>.
 18. Mao X, Yang L, Yu D, Ma T, Ma C, Wang J, Yu Q, Li M. 2021. The vacuole and mitochondria patch (vCLAMP) protein Vam6 is crucial for autophagy in *Candida albicans*. *Mycopathologia* 186:477–486. <https://doi.org/10.1007/s11046-021-00565-x>.
 19. Kroemer G, Levine B. 2008. Autophagic cell death: the story of a misnomer. *Nat Rev Mol Cell Biol* 9:1004–1010. <https://doi.org/10.1038/nrm2529>.
 20. Yeaman MR, Buttner S, Thevissen K. 2018. Regulated cell death as a therapeutic target for novel antifungal peptides and biologics. *Oxid Med Cell Longev* 2018:5473817. <https://doi.org/10.1155/2018/5473817>.
 21. Yun J, Lee DG. 2016. Cecropin A-induced apoptosis is regulated by ion balance and glutathione antioxidant system in *Candida albicans*. *IUBMB Life* 68:652–662. <https://doi.org/10.1002/iub.1527>.
 22. Hwang B, Hwang JS, Lee J, Lee DG. 2011. The antimicrobial peptide, psacothasin induces reactive oxygen species and triggers apoptosis in *Candida albicans*. *Biochem Biophys Res Commun* 405:267–271. <https://doi.org/10.1016/j.bbrc.2011.01.026>.
 23. Hayes BM, Bleackley MR, Wiltshire JL, Anderson MA, Traven A, van der Weerden NL. 2013. Identification and mechanism of action of the plant defensin NaD1 as a new member of the antifungal drug arsenal against *Candida albicans*. *Antimicrob Agents Chemother* 57:3667–3675. <https://doi.org/10.1128/AAC.00365-13>.
 24. Spadari CC, Vila T, Rozental S, Ishida K. 2018. Miltefosine has a postantifungal effect and induces apoptosis in cryptococcus yeasts. *Antimicrob Agents Chemother* 62:e00312-18. <https://doi.org/10.1128/AAC.00312-18>.
 25. Soares JR, José Tenório de Melo E, da Cunha M, Fernandes KVS, Taveira GB, da Silva Pereira L, Pimenta S, Trindade FG, Regente M, Pinedo M, de la Canal L, Gomes VM, de Oliveira Carvalho A. 2017. Interaction between the plant ApDef1 defensin and *Saccharomyces cerevisiae* results in yeast death through a cell cycle- and caspase-dependent process occurring via uncontrolled oxidative stress. *Biochim Biophys Acta Gen Subj* 1861: 3429–3443. <https://doi.org/10.1016/j.bbagen.2016.09.005>.
 26. Aerts AM, François IE, Meert EM, Li QT, Cammue BP, Thevissen K. 2007. The antifungal activity of RsAFP2, a plant defensin from *Raphanus sativus*, involves the induction of reactive oxygen species in *Candida albicans*. *J Mol Microbiol Biotechnol* 13:243–247. <https://doi.org/10.1159/000104753>.
 27. Aerts AM, Bammens L, Govaert G, Carmona-Gutierrez D, Madeo F, Cammue BPA, Thevissen K. 2011. The antifungal plant defensin HsAFP1 from *Heuchera sanguinea* induces apoptosis in *Candida albicans*. *Front Microbiol* 2: 47. <https://doi.org/10.3389/fmicb.2011.00047>.
 28. Eisenberg T, Buttner S, Kroemer G, Madeo F. 2007. The mitochondrial pathway in yeast apoptosis. *Apoptosis* 12:1011–1023. <https://doi.org/10.1007/s10495-007-0758-0>.
 29. Wani MY, Ahmad A, Aqlan FM, Al-Bogami AS. 2021. Citral derivative activates cell cycle arrest and apoptosis signaling pathways in *Candida albicans* by generating oxidative stress. *Bioorg Chem* 115:105260. <https://doi.org/10.1016/j.bioorg.2021.105260>.
 30. Struyfs C, Cools TL, De Cremer K, Sampaio-Marques B, Ludovico P, Wasko BM, Kaerberlein M, Cammue BPA, Thevissen K. 2020. The antifungal plant defensin HsAFP1 induces autophagy, vacuolar dysfunction and cell cycle impairment in yeast. *Biochim Biophys Acta Biomembr* 1862:183255. <https://doi.org/10.1016/j.bbmem.2020.183255>.
 31. Phillips AJ, Sudbery I, Ramsdale M. 2003. Apoptosis induced by environmental stresses and amphotericin B in *Candida albicans*. *Proc Natl Acad Sci U S A* 100:14327–14332. <https://doi.org/10.1073/pnas.2332326100>.
 32. Li LR, Sun J, Xia SF, Tian X, Cheserek MJ, Le GW. 2016. Mechanism of antifungal activity of antimicrobial peptide APP, a cell-penetrating peptide derivative, against *Candida albicans*: intracellular DNA binding and cell cycle arrest. *Appl Microbiol Biotechnol* 100:3245–3253. <https://doi.org/10.1007/s00253-015-7265-y>.
 33. Liao H, Liu S, Wang H, Su H, Liu Z. 2019. Enhanced antifungal activity of bovine lactoferrin-producing probiotic *Lactobacillus casei* in the murine model of vulvovaginal candidiasis. *BMC Microbiol* 19:7. <https://doi.org/10.1186/s12866-018-1370-x>.
 34. Rossi DC, Muñoz JE, Carvalho DD, Belmonte R, Faintuch B, Borelli P, Miranda A, Tabora CP, Daffre S. 2012. Therapeutic use of a cationic antimicrobial peptide from the spider *Acanthoscurria gomesiana* in the control of experimental candidiasis. *BMC Microbiol* 12:28. <https://doi.org/10.1186/1471-2180-12-28>.
 35. Liao H, Liu S, Wang H, Su H, Liu Z. 2017. Efficacy of Histatin5 in a murine model of vulvovaginal candidiasis caused by *Candida albicans*. *Pathog Dis* 75:ftx072. <https://doi.org/10.1093/femspd/ftx072>.
 36. Piotrowska U, Sobczak M, Oledzka E. 2017. Current state of a dual behaviour of antimicrobial peptides—therapeutic agents and promising delivery vectors. *Chem Biol Drug Des* 90:1079–1093. <https://doi.org/10.1111/cbdd.13031>.
 37. Mookherjee N, Anderson MA, Haagsman HP, Davidson DJ. 2020. Antimicrobial host defence peptides: functions and clinical potential. *Nat Rev Drug Discov* 19:311–332. <https://doi.org/10.1038/s41573-019-0058-8>.
 38. Berman J. 2006. Morphogenesis and cell cycle progression in *Candida albicans*. *Curr Opin Microbiol* 9:595–601. <https://doi.org/10.1016/j.mib.2006.10.007>.
 39. Mayer FL, Wilson D, Hube B. 2013. *Candida albicans* pathogenicity mechanisms. *Virulence* 4:119–128. <https://doi.org/10.4161/viru.22913>.
 40. Zhu D, Chen F, Chen YC, Peng H, Wang KJ. 2021. The long-term effect of a nine amino-acid antimicrobial peptide AS-hepc3_(48–56) against *Pseudomonas aeruginosa* with no detectable resistance. *Front Cell Infect Microbiol* 11:752637. <https://doi.org/10.3389/fcimb.2021.752637>.
 41. Guilhelmelli F, Vilela N, Smidt KS, de Oliveira MA, da Cunha Moraes Álvares A, Rigonatto MCL, da Silva Costa PH, Tavares AH, de Freitas SM, Nicola AM, Franco OL, Derengowski LdS, Schwartz EF, Mortari MR, Bocca AL, Albuquerque P, Silva-Pereira I. 2016. Activity of scorpion venom-derived antifungal peptides against planktonic cells of *Candida* spp. and *Cryptococcus neoformans* and *Candida albicans* biofilms. *Front Microbiol* 7:1844. <https://doi.org/10.3389/fmicb.2016.01844>.
 42. Hao B, Cheng S, Clancy CJ, Nguyen MH. 2013. Caspofungin kills *Candida albicans* by causing both cellular apoptosis and necrosis. *Antimicrob Agents Chemother* 57:326–332. <https://doi.org/10.1128/AAC.01366-12>.
 43. Liand JN, Yany L, Zhao T, Liu YW. 2015. Comparison and optimization of the conventional methods for yeast sample preparation for transmission electron microscopy. *J Chin Electr Microsc Soc* 34:85–88.
 44. Wu XZ, Chang WQ, Cheng AX, Sun LM, Lou HX. 2010. Plagiochin E, an antifungal active macrocyclic bis(bibenzyl), induced apoptosis in *Candida albicans* through a metacaspase-dependent apoptotic pathway. *Biochim Biophys Acta* 1800:439–447. <https://doi.org/10.1016/j.bbagen.2010.01.001>.
 45. Fidel PL, Jr, Cutright J, Steele C. 2000. Effects of reproductive hormones on experimental vaginal candidiasis. *Infect Immun* 68:651–657. <https://doi.org/10.1128/IAI.68.2.651-657.2000>.